Vorticity Measurements in Turbulent Soap Films

H. Kellay,[1] X. L. Wu,[2] and W. I. Goldburg[2]
[1]*Centre de Physique Moleculaire Optique et Hertzienne, Universite Bordeaux I, 351 Cours de la Liberation, 33405 Talence Cedex, France*
[2]*Department of Physics and Astronomy, University of Pittsburgh, Pittsburgh, Pennsylvania 15260*
(Received 10 July 1997)

Measurements of vorticity fluctuations are carried out in rapidly flowing turbulent soap films driven by gravity. Isotropic turbulence is generated by inserting one-dimensional grids through the film. The vorticity fluctuations are measured using two optical-fiber velocimeters capable of measuring the fluctuations of both the longitudinal and transverse components of the velocity simultaneously. Our results indicate scaling of the vorticity spectrum, yet this scaling is different from what is predicted theoretically.
[S0031-9007(97)04569-9]

PACS numbers: 47.27.Gs, 67.40.Vs, 92.60.Ek

Measurements of vorticity fluctuations in turbulent flows is remarkably difficult and few if any measurements have been attempted [1]. Here we present measurements of vorticity spectra in a turbulent soap film flowing between two parallel wires under the action of gravity. These films are sufficiently thin (thickness of a few micrometers) that the velocity vector is confined to the plane of the film and the vorticity is perpendicular to this plane. We here take advantage of the two dimensionality of the flow in these films and use a recently developed optical fiber velocimeter to measure the two components of the velocity vector at two different locations simultaneously. The Taylor frozen turbulence assumption, which assumes that the small-scale eddies are swept by the mean flow past the observation point without suffering much change, is used to obtain the velocity at two other locations and the vorticity is constructed from the velocities at the four points.

Two-dimensional (2D) turbulence is very different from three-dimensional (3D) turbulence; the conservation of both energy and enstrophy or mean-square vorticity in 2D turbulence introduces additional constraints on energy transfers between different spatial scales [2,3]. In 3D turbulence the phenomenological theory of Kolmogorov predicts an energy cascade from large scales to small scales and a scaling law for the energy density spectrum $E(k) = k^{-b}$ with $b = 5/3$. In 2D turbulence, similar phenomenological theories predict an inverse energy cascade from the injection scale to larger scales and a direct enstrophy cascade to smaller scales. The scaling law for the energy density spectrum is the same as in 3D but only for scales larger than the injection scale. For scales smaller than the injection scale, the energy density spectrum is different and has the exponent $b = 3$ while the enstrophy density spectrum is predicted to scale as $e(k) = k^{-c}$ with $c = 1$. By definition $\int e(k)\,dk = \frac{1}{2}\langle\omega^2\rangle$, where ω is the vorticity, $k = \sqrt{k_x^2 + k_y^2}$, and the brackets designate a spatial average.

Few ways are known to produce isotropic 2D turbulence in the laboratory; one of them uses rapidly flowing soap films. The use of soap films in the study of quasi-2D hydrodynamics has been pioneered by Couder and coworkers [4], and Gharib and Derango [5]. In a subsequent study of ours, measurements of velocity differences and velocity power spectra showed that the properties of turbulence generated behind one-dimensional (1D) grids in a soap film channel driven by gravity are in reasonable agreement with the existence of an enstrophy cascade from large scales to small scales. However, no evidence of an inverse energy cascade was seen [6]. Some evidence of the existence of the inverse cascade in 2D turbulence was reported by Gharib and Derango [5] and by Sommeria [7].

The soap film channel used for this study was developed recently to investigate the properties of turbulence behind 1D grids (combs) inserted through the film [6], and has been refined considerably to study laminar flow [8]. The flow behind grids in such a channel was already studied using homodyne correlation spectroscopy (HCS). Also single-point measurements of 1D velocity spectra were made using a novel optical fiber velocimeter. The first method measures the symmetric part of the probability distribution function of velocity differences between two points separated by a distance ℓ, while the second method gives the instantaneous velocity vector. It was found that in such a channel, isotropic turbulence could be generated behind a 1D grid inserted through the film. The transverse velocity differences between two points separated by a distance ℓ, as measured by HCS, were found to scale linearly with this distance for $0.5 < \ell < 4$ mm. The 1D power spectra for both the longitudinal and the transverse components were also found to scale with the frequency f or the wave number k_y, where the flow, of mean speed $\bar{V}$, is in the $+y$ direction as shown in Fig. 1. The wave vector component k_y is related to f through the frozen turbulence assumption: $k_y = 2\pi f/\bar{V}$. The energy density spectrum was found to scale as the wave number to a power of roughly 3.5. Our measurements were in reasonable agreement with theories predicting an enstrophy cascade to small scales in 2D turbulent flows [3,6]. The mean-square vorticity or enstrophy spectra we report here will be compared to what is expected for 2D isotropic turbulence in the enstrophy cascade range

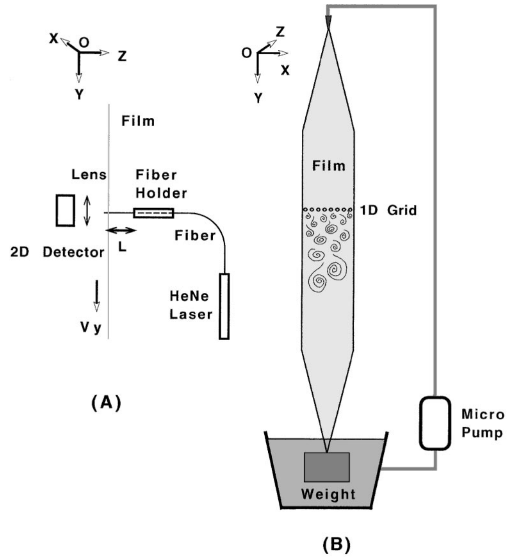

FIG. 1. (a) A schematic of the fiber setup. The fiber penetrates the film for less than 0.5 mm and its length measured from the fiber holder is 6 mm. (b) A schematic of the soap film channel setup. Using a micropump the film is constantly replenished with soap solution. The frame of the channel is nylon wire of diameter 0.08 cm. The width of the channel was 6 cm and its length is 200 cm.

of scales. If the turbulence is isotropic and the fluid is incompressible, then the enstrophy spectrum $e(k)$ is uniquely related to the $E(k)$ through the equation $e(k) = k^2E(k)$ (see Chap. 5 of Ref. [3]).

The channel used for this experiment has a length of 2 m and a width W of 6 cm. A schematic of the setup is shown in Fig. 1. Soapy water was pumped from a reservoir to the top of the channel with a variable speed micropump which has a range of flow rates $\langle J \rangle$ from less than 0.1 to 1 ml/s. Estimating the mean film thickness $\langle h \rangle$ as 3 μm and using the above range of flow rates, $\bar{V}(= \langle J \rangle / W\langle h \rangle)$ falls in the range between 0.5 and 4 m/s. We used a commercial detergent at a concentration of about 2% in water for the soap solution. The channel frame was made of nylon wires of diameter 0.8 mm, which were draped over hooks for support with a weight suspended at its bottom end to tighten the frame. The soap film obtained with this method is sufficiently robust to last several hours without breaking. The flow in this channel was studied recently, and a laminar flow regime was found and characterized [8].

To produce turbulent flow, a comb or 1D grid is inserted through the film. The teeth of the comb are equally spaced, with a separation distance of 6.5 mm, and the diameter of each tooth is 3.5 mm. For locations a few centimeters below the grid, isotropic turbulence can be obtained. These are the locations at which the vorticity spectra are measured.

Each velocimeter consists of an optical fiber, one end of which penetrates about 0.5 mm through the film and which is deflected by the film flow. The distance L between the fiber tip and the fiber holder is 6 mm, as shown in Fig. 1. The output of a small laser is connected to the far end of the fiber, producing a somewhat diffuse spot at the deflecting end. The $x(t)$ and $y(t)$ deflections of this spot are measured by a position-sensitive detector and recorded in a computer. Independent measurements establish that the vertical deflection is proportional to the y component of the velocity. This linearity of the fiber response requires that one is below the resonance frequency f_0 of the fiber deflection. The proportionality of deflection and local velocity depends on the fact that the thickness of the film $h(t)$ deviates only slightly from its mean value $\langle h \rangle$. With the fibers used here, diameter $=$ 60 μm, f_0 was 1.5 kHz.

To measure vorticity fluctuations we use two velocity probes at the same vertical position and separated horizontally by a small distance Δx (typically 1 mm) to measure the velocity in two different points in the flow. The vorticity is constructed from the measured velocity in two different locations: both components of the velocity are needed at different positions simultaneously, since the vorticity is given by $\omega = dv_y/dx - dv_x/dy$, where v_x and v_y are, respectively, the transverse and longitudinal components of the velocity. In the above equation, the first derivative term, for a small horizontal separation between the two probes, is taken as the difference between the longitudinal velocities at the two horizontal points. The other derivative term is constructed using the frozen turbulence assumption: the transverse component is measured at time t and time $t + \Delta t$ such that $\bar{V}\Delta t = \Delta y = \Delta x$ and the spatial derivative dv_x/dy is taken as $[v_x(t + \Delta t) - v_x(t)]/\bar{V}\Delta t$. Denoting the four velocities, two for each point are recorded as (v_{x1}, v_{y1}) and (v_{x2}, v_{y2}), and the vorticity is evaluated as

$$\omega = \frac{1}{2}[v_{y2}(t) - v_{y1}(t) + v_{y2}(t + \Delta t) - v_{y1}(t + \Delta t)]/\Delta x - \frac{1}{2}[v_{x1}(t + \Delta t) - v_{x1}(t) + v_{x2}(t + \Delta t) - v_{x2}(t)]/\bar{V}\Delta t \,.$$

For these measurements the two probes must have the same response and therefore the same resonance frequency f_0. We use two fibers with the same diameter 60 μm, the same length L, and the same penetration length through the film. We checked that small differences between the resonance frequencies of the fibers did not affect the results but this difference was minimized as much as possible. Also small variations of the horizontal separation did not change the results either.

The horizontal separation Δx of the two fibers was typically between 1 and 0.7 mm which are orders of magnitude larger than the amplitude of the fluctuation at the tip. The interval Δt used was between 0.5 and 0.33 ms for speeds between 200 and 300 cm/s. The four signals from the position detectors were connected to an analog-to-digital (A/D) converter and could be read almost simultaneously. The time delay between consecutive channels was fixed by the A/D board hardware and was 2 μs. The four signals were then sampled at a frequency f_s fixed by the time interval Δt: $(f_s = 1/\Delta t)$ and was typically between 2000 and 3000 Hz. The time delay between two consecutive signals is much smaller than the interval Δt. This allows us to consider that the four signals are measured almost simultaneously.

We first measured the velocity fluctuations $v_x(t)$ and $v_y(t)$ at a point Y several centimeters below the grid. This is roughly the same position where the vorticity spectra $\langle|\omega(f)|^2\rangle$ were subsequently measured. Figure 2 shows such a measurement for a flow rate of 0.6 ml/s. The spectra $S_{xx}(f) = \langle|v_x(f)|^2\rangle$ and $S_{yy}(f) = \langle|v_y(f)|^2\rangle$ of the transverse and the longitudinal velocities have the same amplitude for most of the frequency range probed except at low frequencies where the transverse velocity spectrum decreases as the frequency decreases. The bracket in all of the experimental measurements indicate a time average. This shows that the flow is isotropic at small scales ranging from a few centimeters down to a few millimeters but is anisotropic at larger scales. At high frequencies both components show a scaling range where $S_{xx}(f)$ and $S_{yy}(f)$ are proportional to $f^{-\gamma}$ with γ close to 3. A line with this slope appears in the figure. This value of γ is consistent with freely decaying 2D turbulence [9]. The spectrum shown here is typical for high flow rates at locations between 3 and 8 cm behind the grid. This is the region where the vorticity is measured. The appearance of the fiber resonance is the source of the rise in the S_{xx} and S_{yy} near $f \simeq 800$ Hz.

The measured enstrophy spectra $e(f) = \langle|\omega(f)|^2\rangle$ are shown in Fig. 3 for a high flow rate at two different distances from the grid. Spectrum (a) is taken at $Y = 5$ cm at a flow rate of 0.68 ml/s. Spectrum (b) is taken at $Y = 7$ cm at a flow rate of 0.75 ml/s. The spectra are broadband showing that the flow presents a continuum of modes which is a characteristic of turbulent flows. The anomalous two points at low frequency regime are due to vibrations of the experimental setup. Note also that the spectra flatten at frequencies below 50 Hz corresponding to a length scale of about 4 cm, which is comparable to the channel width of 6 cm. At frequencies above 60 Hz the spectra show a decrease as the frequency increases. This decay of the amplitude can be approximated by a power law for about a decade between 60 and 500 Hz. In Fig. 4(a), enstrophy power spectra are shown for a location of 5 cm behind the grid but for a series of flow rates. For small flow rates (less than 0.4 ml/s) the amplitude of the vorticity power spectrum decreases rapidly for frequencies between 40 and 200 Hz. For these flow rates there is little high frequency dynamics and the spectrum flattens at frequencies above 200 Hz. As the flow rate increases, $e(f)$ increases and the scaling appears more clearly, extending to higher frequencies at flow rates above 0.4 ml/s. Nearly identical results are obtained at other locations behind the grid as can be seen in Fig. 4(b) for

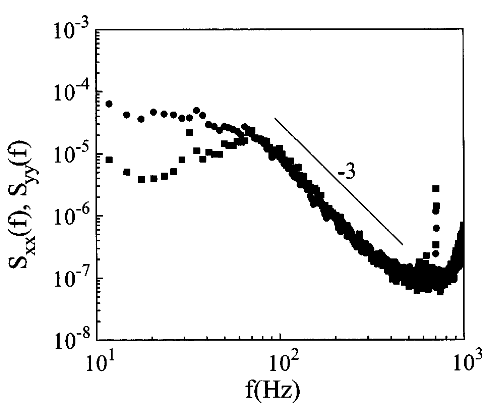

FIG. 2. Longitudinal (filled circles) and transverse (filled squares) velocity power spectra measured at distance $Y = 6$ cm below the grid. The flow rate is 0.6 ml/s. Isotropy is clearly seen at high frequencies corresponding to small wavelength velocity fluctuations. The line has a slope of -3.

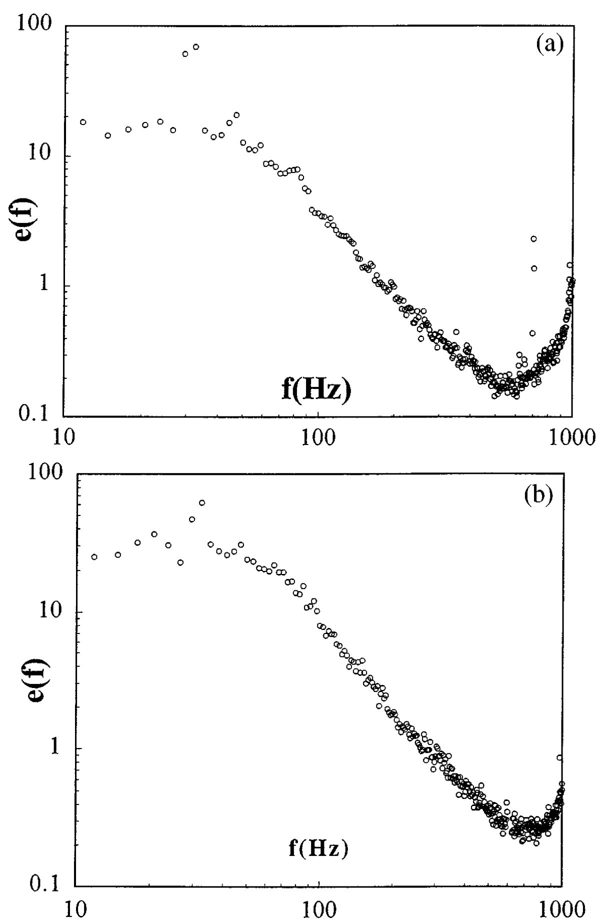

FIG. 3. (a) Vorticity power spectrum behind a 1D grid measured at $Y = 5$ cm and with a flow rate of 0.68 ml/s. (b) Vorticity power spectrum measured at $Y = 7$ cm and with a flow rate of 0.75 ml/s.

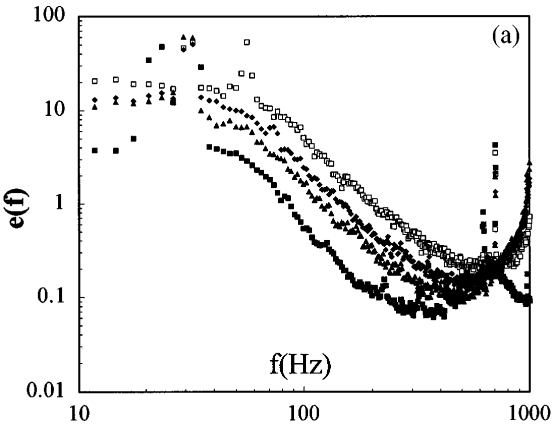

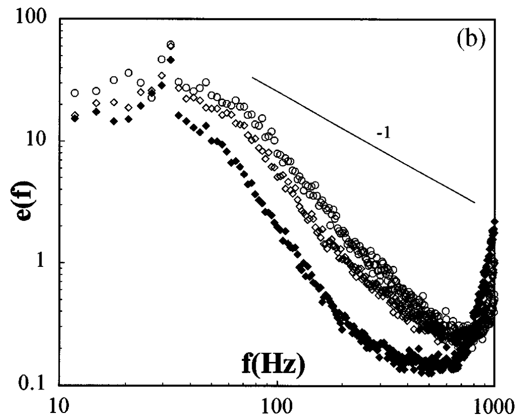

FIG. 4. (a) Vorticity power spectra behind the grid at a distance $Y = 5$ cm. The flow rates are 0.2 ml/s (filled squares), 0.4 ml/s (filled triangles), 0.68 ml/s (diamonds), and 0.8 ml/s (open squares). (b) Vorticity power spectra at a distance $Y = 7$ cm from the grid. The flow rates are 0.4 ml/s (diamonds), 0.55 ml/s (open diamonds), and 0.75 ml/s (circles). The straight line has the canonical slope of unity.

$Y = 7$ cm. Quantitatively, the vorticity spectrum decays as $\langle|\omega(f)|^2\rangle \sim f^{-c}$, with c close to 2. The results are robust as they can be reproduced at different locations in the flow and with different flow rates.

At sufficiently high injection rates, the flow is turbulent and self-similar as indicated by the scaling of both velocity and vorticity power spectra. By using the frozen turbulence assumption to convert frequency to wave number ($k_y = 2\pi V/f$), the 1D enstrophy spectrum is found to scale as $e(k_y) = \langle\omega^2(k_y)\rangle = k_y^{-c}$ with c falling between 1.8 and 2.2. Theoretically a value of 1 is expected for c in the enstrophy cascade range of scales. The straight line in Fig. 4 has a slope of unity.

The measured exponent c differs considerably from the theoretical prediction. In some numerical simulations of decaying 2D turbulence the enstrophy spectrum was calculated and its scaling also appears to differ from the theoretical prediction [10]. In our case several reasons can be invoked to explain this effect. The main effect is the compressibility of the flow since the soap film can sustain thickness fluctuations; this has been noted in stratified flows [11]. This issue raises the question of the coupling between the velocity and the thickness fluctuations of the film and can be addressed by a direct study of the thickness field, a subject which we are currently investigating.

Another factor is the validity of the frozen turbulence assumption which is used extensively here. In our previous study of turbulence in flowing soap films we had compared measurements using two techniques: one of them (optical fiber velocimetry) used the frozen turbulence assumption while the other one (HCS) did not. The results we reported were in reasonable agreement with each other for small scales (0.05 to 0.4 cm) which suggests that the use of the frozen turbulence assumption for small scales is acceptable; however, for scales larger than a few millimeters, the use of this assumption may still be problematic. The other interesting possibility is that 2D turbulence is highly anomalous (or intermittent), giving rise to scaling exponents which are different from the phenomenologically predicted ones.

In conclusion, we have presented one of the first studies of vorticity fluctuations in a turbulent soap film flow. We have introduced a new technique for the measurement of vorticity fluctuations in 2D flows which takes advantage of the two dimensionality of the flow and of a recently developed optical fiber velocimeter capable of measuring the two components of the velocity simultaneously. The measurements show that the velocity and the vorticity are self-similar in the range of scales from a few millimeters to a few centimeters. The scaling exponent measured for the vorticity power spectrum differs from the theoretically expected one.

This work was supported by grants from Conseil Regional d'Aquitaine, and the NSF under Grants No. DMR 9424355 and No. INT 9603361.

[1] M. B. Frish and W. W. Webb, J. Fluid Mech. **107**, 173 (1981).
[2] R. Kraichnan, Phys. Fluids **10**, 1417 (1967); G. K. Batchelor, Phys. Fluids Suppl. II **12**, 233 (1969).
[3] M. Lesieur, *Turbulence in Fluids* (Kluwer Academic Publishers, Dordrecht, 1990), 2nd ed.
[4] Y. Couder, J. Phys. (Paris), Lett. **45**, L-353 (1984); Y. Couder, J. M. Chomaz, and M. Rabaud, Physica (Amsterdam) **37D**, 384 (1989).
[5] M. Gharib and P. Derango, Physica (Amsterdam) **37D**, 406 (1989).
[6] H. Kellay, X-l. Wu, and W. I. Goldburg, Phys. Rev. Lett. **74**, 3975 (1995).
[7] J. Sommeria, J. Fluid Mech. **170**, 139 (1986).
[8] M. Rutgers, X-l. Wu, R. Bagavatula, A. A. Petersen, and W. I. Goldburg, Phys. Fluids **8**, 2847 (1997).
[9] J. R. Chasnov, Phys. Fluids **9**, 171 (1997).
[10] W. H. Matthaeus, W. T. Stribling, D. Martinez, S. Oughton, and D. Montgomery, Phys. Rev. Lett. **66**, 2731 (1991).
[11] C. T. Yap and C. W. van Atta, Dyn. Atmos. Oceans **19**, 289 (1993).